applied sciences

MDPI

Article

Model Based Open-Loop Wind Farm Control Using Active Power for Power Increase and Load Reduction

Hyungyu Kim, Kwansu Kim and Insu Paek *

Department of Advanced Mechanical Engineering, Kangwon National University, Chuncheon-si 24341, Gangwon-do, Korea; khg0104@kangwon.ac.kr (H.K.); kwansoo@kangwon.ac.kr (K.K.)

* Correspondence: paek@kangwon.ac.kr; Tel.: +82-33-250-6379

Received: 2 August 2017; Accepted: 11 October 2017; Published: 16 October 2017

Abstract: A new wind farm control algorithm that adjusts the power output of the most upstream wind turbine in a wind farm for power increase and load reduction was developed in this study. The algorithm finds power commands to individual wind turbines to maximize the total power output from the wind farm when the power command from the transmission system operator is larger than the total available power from the wind farm. To validate this wind farm control algorithm, a relatively high fidelity wind farm simulation tool developed in the previous study was modified to include a wind farm controller which consists of a wind speed estimator, a power command calculator and a simplified wind farm model. In addition, the wind turbine controller in the simulation tool was modified to include a demanded power tracking algorithm. For a virtual wind farm with three 5 MW wind turbines aligned with the wind, simulations were performed with various ambient turbulent intensities, turbine spacing, and control frequencies. It was found from the dynamic simulation using turbulent winds that the proposed wind farm control algorithm can increase the power output and decrease the tower load of the most upstream wind turbine compared with the results with the conventional wind farm control.

Keywords: wind farm control; wind farm model; function minimization; power increase

1. Introduction

Offshore wind farms using fixed substructures are mostly constructed in seawaters having a depth of less than 40 m, and this often limits the number of wind turbines that can be installed in a wind farm. The spacing between wind turbines commonly range from 7 RD to 11 RD, where RD represents the rotor diameter of the wind turbine [1,2]. Considering the fact that the rotor diameters of modern wind turbines commonly reach 100 m, the spacing between wind turbines seems large but it is still necessary to reduce the wake effects from upstream wind turbines on downstream ones which result in lower power and higher load [3].

Investigations on active induction wind farm control to reduce the wake strength by regulating the power of the upstream wind turbines less than their available power have been done by researchers. Earlier research articles were focused on the phenomenon itself, and the physical explanations of the power increase using one-dimensional momentum theory were presented [4,5]. The simple model predicted an increase of 4.1% of the total power of two turbines in line when the induction of the first wind turbine was reduced from 1/3 to 1/5. In addition, to prove the idea, wind tunnel tests with micro scale wind turbine model arrays with manually adjustable blade pitches with a turbine spacing of 4.5 RD were used. From the scaled farm measurements, about 4.5% of increase in the total power was observed with a blade pitch angle of 2°. However, later, the measurement uncertainty turned out to be greater than the power increase 6%, and the results were also found to be greatly affected by the Reynolds number effects occurring only in wind tunnel tests [5,6]. In addition, a few

field measurements with multi-MW wind turbines with a 3.8 RD spacing were tried but not very successful [5,6] to make a quantitative conclusion. Later, the field data were reanalyzed for two 2.5 MW wind turbines with a spacing of 3.8 RD, and turned out to have a power increase of about 5% with a fixed pitch angle of 2° [7].

After that, the active induction wake control method based on the manual blade pitch adjustment (change of axial induction) was applied to a simple wind turbine model with an engineering wake model. The simulation concluded that the adjustment of the blade pitch angle can increase the total power of a wind farm by about 10% [8–10].

Later, articles focused on various wind farm control algorithms including genetic algorithms were presented [11–14]. Some were wind farm model based methods and some were model free methods. Because it is very hard to prove the wind farm control effects on the farm power output in real wind farms, all validations were made with simulations. In addition, the facts that a wind farm simulation must deal with multiple wind turbines, and simulations with multiple wind turbines require large computational loads, limited the simulations to be the simulations of simple wind turbine models without any dynamics in conjunction with a simple wake model. The wind turbine models were simply algebraic equations with power coefficient and the simulations were made with constant wind speeds and no turbulence. The power gains from these simplified static analyses varied from 0.6% to 25% depending on the control method [11–14]. In addition, some researchers tried to change the wind turbine operating point to reduce the wake effect based on simple wind turbine models with engineering wake models and they concluded with power increases of 1.86% to 6.24% [8]. However, the results are considered to be exaggerated due to the simple wind turbine model and the constant wind.

Recently, an extremum seeking control as a model-free method was used to prove the algorithm. The simulation was done in turbulent winds with a few different turbulence intensities [15] but the wind turbine model was still a simple algebraic equation that does not have any system dynamics. In the study, the controller was successful with low turbulence intensity. However, the controller failed with high turbulence intensity which was about 0.21. This was because, with high turbulence intensity, the controller could not distinguish power variations due to wind speed change from those due to wind farm control.

More recently, the concept of power increase by regulating the power of the most upstream wind turbine was reinvestigated with a relatively high fidelity wind farm simulation model [16]. In the research, it was found that the power partialization percentage, defined as the power output to the available power of the most upstream wind turbine to achieve the maximum power of a wind farm, is a function of the wind turbine spacing but is not much affected by the wind speed. Therefore, the power regulation of the upstream wind turbine for power maximization is achieved not by a constant blade pitch angle but by a constant power partialization of the most upstream wind turbine. This means that the blade pitch angle of the most upstream wind turbine must be adjusted when the wind speed varies. In the study, a power increase of 4.1% was observed with ten wind turbines in series with a spacing of 4 RD when the partialization of the most upstream wind turbine was 0.825. However, in that study, the wind was not a turbulent wind but a constant wind, and the study did not include any wind farm control algorithm, but did include results with manual power adjustments of the most upstream wind turbine for better understanding of power increase mechanism.

There have also been conflicting results in the literature that the active induction of the most upstream wind turbine does not increase the overall power output from the wind farm [17,18]. They are mostly based on the simulation results with the LES (Large Eddy Simulation) method. Nilsson et al. [17] applied the LES to simulate the Lillgrund wind farm and showed the simulation results with the ambient turbulence intensity of 5.6% that the manual blade pitching of the first wind turbine by multiples of 2° does not increase the total power. However, in their study, the wind turbine dynamic and control was not considered. In addition, Annoni et al. [18] applied the high fidelity simulation tool, SOWFA (Simulation fOr Wind Farm Applications) to investigate the power increase of a small wind farm of five wind turbines by power curtailment. However, the manual

blade pitching of the most upstream wind turbine did not increase the total farm power, but rather decreased it approximately by 8.9%. In their simulation results with five wind turbines in series, the powers of all four wind turbines except the fifth one decreased with the power curtailment of the most upstream wind turbine. They concluded that for the total power increase, a suitable wind farm control is necessary. Goit and Meyers [19] applied an optimal control strategy to the LES simulation with an actuator disk model to investigate the total power increase of a wind farm with 50 wind turbines. Unlike other LES simulations with the fixed blade pitching, they found the power increase of 16% compared with the uncontrolled case. However, the wind turbine dynamics and power control algorithms of wind turbines including blade pitch (most upstream wind turbine only) and generator torque (all wind turbines) controls were not considered in their study.

In this study, the previous study [16] was further expanded to develop a model based wind farm control method with a simple but effective open-loop wind farm control algorithm based on a function minimization method. The command from the wind farm controller to the wind turbine was the active power of the wind turbine and the wind farm control algorithm was validated with the relatively high fidelity wind farm model constructed previously [20] but modified for this study. The originality of this study compared with the previous research can be summarized by the following factors.

First, the proposed wind farm control in this study considered implementation of the control in actual wind farm controllers that receive data from wind turbines and give commands to them without affecting the built-in wind turbine torque and pitch control algorithm for maximum power point tracking and power regulation. By considering the fact that modern multi-megawatt wind turbine controllers use the torque and rotating speed of the generator as targets to achieve power maximization or regulation, the variable of the most upstream wind turbine used for a wind farm control was chosen not to be the blade pitch angles or axial induction factors that used for the previous articles [3–15] but to be the generator power. The generator power can be expressed as the torque multiplied by the rotating speed of the generator, and, therefore, the power regulation of the most upstream wind turbine could be done without affecting its built-in control algorithm. However, the wind turbine controller of the wind turbine model in the wind farm simulation tool had to be modified to additionally include a demanded power tracking control algorithm.

Second, by considering the fact that the optimal power partialization of the most upstream wind turbine is not much affected by the wind speed [16], a simple open loop control with power command output to wind turbines was implemented to the wind farm controller. Modern multi-megawatt wind turbines already use open-loop control for maximum power point tracking when the wind speed is lower than the rated wind speed [21–23]. In addition, a simple open-loop dispatch wind farm control based on the available powers of the wind turbines in a wind farm is already implemented for a power demand tracking in wind farms. Therefore, a simple but effective open-loop wind farm control for a total power increase in a farm was not new in this area and was chosen for this study. The proposed wind farm controller consists of a wind speed estimator, optimal power command calculator and a wind farm model. It calculates the available power at a chosen control frequency, finds the optimal power commands to individual wind turbines based on its wind farm model, and sends the commands to wind turbines for power increase and load reduction.

Thirdly, the proposed wind farm control algorithm was validated not with a simple model without any dynamics under steady wind but with a high fidelity wind farm simulation tool under turbulent wind with wind turbine dynamics and controls. For this, the wind turbine controller for power command tracking as well as the wind farm controller were constructed and implemented to the high fidelity simulation tool [16]. Therefore, more realistic simulation results can be obtained compared to the previous studies [4–19] for the validation of the proposed wind farm control algorithm.

2. Methodology

2.1. Wind Farm Simulation Tool

For simulations, a wind farm simulation tool, which was constructed in the previous study, was modified to have communications with the wind farm controller. The wind farm controller has a control algorithm based on a simplified farm model embedded in the controller and performs a model predictive control. The simulation tool is originally based on SimWindFarm [24] but modified to have Ainslie's eddy viscosity wake model and new wind turbine and farm controllers [20,25]. It consists of individual wind turbine models, wake model, wind propagation model, and wind generator, as shown in Figure 1.

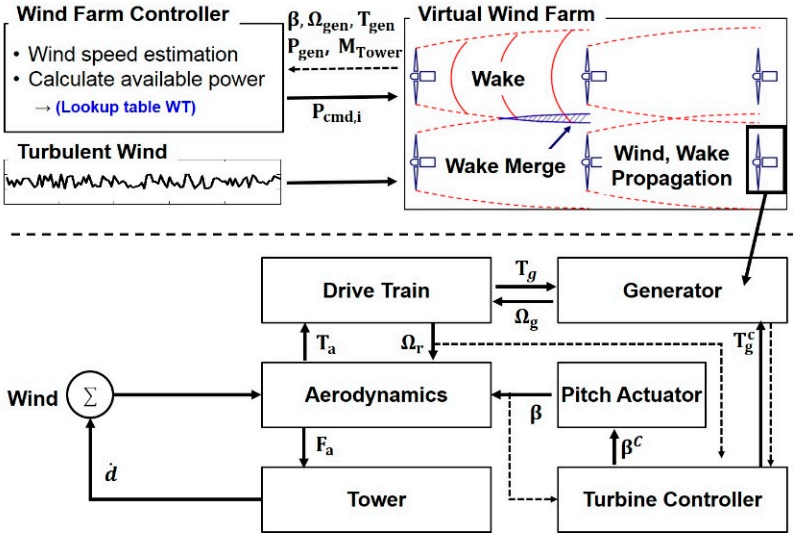

Figure 1. Schematic of wind farm model used for simulation including wind turbine and farm control.

The simulation tool was coded with C language to achieve short simulation time. It can simulate the load variation of a wind turbine for different wind turbine states subjected to different winds, but still the wind propagation is dependent on the Taylor's frozen turbulence assumption. The individual wake fields generated by wind turbines are combined to be applied to downstream wind turbines with the "Sum of Squares of Velocity Deficit" equation. The equation is used for a well-known commercial wind farm design tool [26] and is shown in Equation (1).

$$\text{Deficit}_n = \sqrt{\sum_{k=1}^{n-1} (\text{Deficit}_{kn})^2} \tag{1}$$

The "Sum of Squares of Velocity Deficit" equation shown in Equation (1) is also known as the quadratic sum model, where k represents the total number of turbines constituting the wind farm and n represents the number of upstream wind turbines that make a wake effect on them [27]. The wind speed deficit in Equation (1) is defined as

$$\text{Deficit} = \frac{\Delta U}{U_\infty} \tag{2}$$

where ΔU means the difference between the freestream wind speed and the wind speed in the wake region, and U_∞ means the freestream wind speed.

The wind turbine model is a combination of first or second order dynamic sub-models [28] and simulates wind turbine power output and tower loads dynamically for turbulent winds. The model

receives wind speed and power command from a wind farm controller and calculates electrical power, blade pitch angle, generator speed, and the tower load. The simplified order sub models include drive-train model, generator model, pitch actuator model, tower model, and controller model. The aerodynamic conversion is calculated in an aerodynamic model which is a three-dimensional look-up table with a function of blade pitch angle and tip speed ratio obtained from a commercial wind turbine dynamic simulation tool. The wind turbine controller includes a basic torque and collective pitch control with a power demand tracking to achieve power output commanded from a wind farm controller. The validation of the dynamic wind turbine model was made in the previous study [20].

2.2. Wind Farm Controller

The wind farm controller constructed and imbedded to the wind farm simulation tool in this study means a supervisory controller that collects wind turbine states and sends commands to individual wind turbines to maximize the farm power output. It receives the blade pitch angle, generator speed and electrical power from individual wind turbines and sends power command to individual turbines.

The wind farm controller consists of a wind speed estimator, a power command calculator, and a wind farm model. Figure 2 is a block diagram of the relation between the simulation tool for the verification of the control algorithm and the wind farm developed through this study.

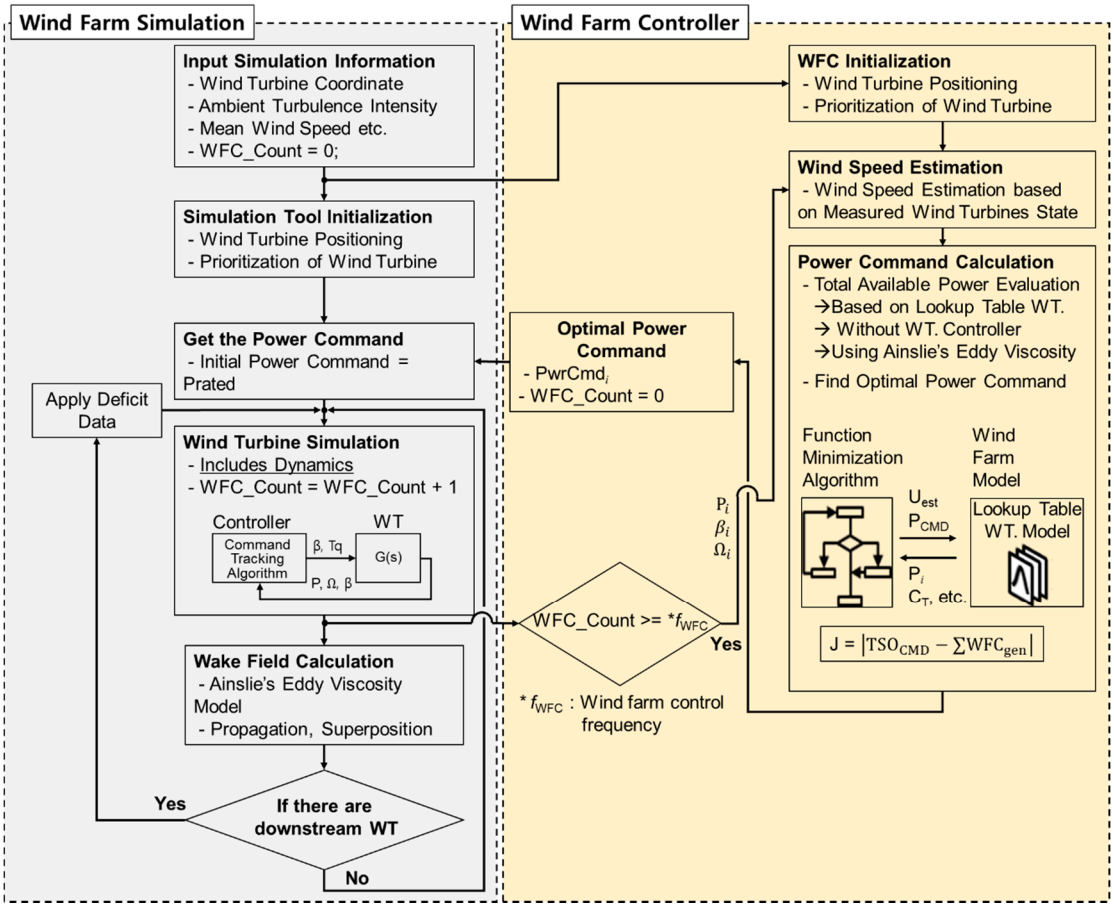

Figure 2. Structure of wind farm controller.

The wind speed estimator estimates the averaged wind speeds at the rotor center of individual wind turbines from the known properties and measured signals from wind turbines. Firstly, it calculates the aerodynamic torque from Equation (3) which is a two-mass model equation of motion for the drive train available in the literature [28].

$$\left(J_r + N^2 J_g\right)\frac{\mathrm{d}\dot{\theta_r}}{\mathrm{d}t} = \mathrm{T}_a - N\mathrm{T}_g - \left(\mathrm{B}_r + N^2\mathrm{B}_g\right)\dot{\theta_r} \tag{3}$$

In Equation (3), J is the mass moment of inertia, N is the gear ratio, $\dot{\theta_r}$ is the rotational speed, T is the torque, B is the damping coefficient, and $\mathrm{d}/\mathrm{d}t$ is the time derivative. In addition, the subscripts r, g, and a represent rotor, generator and aerodynamic, respectively. After finding the aerodynamic torque, T_a, from Equation (3), the averaged wind speed V is obtained from Equation (4) [29].

$$\mathrm{T}_a = \frac{1}{2}\rho\pi\mathrm{R}^3\left(\frac{C_P(\lambda,\beta)}{\lambda}\right)V^2 \tag{4}$$

In Equation (4), ρ is the density of air, R is the rotor radius, C_P is the power coefficient, λ is the tip speed ratio, β is the pitch angle, and V is the averaged wind speed.

The power command calculator from the wind farm controller calculates available powers of the wind turbines based on the estimated wind speed obtained using Equations (3) and (4) by using

$$\mathrm{P}_{av} = \mathrm{T}_a \cdot \dot{\theta_r} \cdot \eta_m \cdot \eta_g \tag{5}$$

where P is the electrical power, and η is the efficiency. The subscripts av, and m represent available and mechanical, respectively [21].

The power command calculator of the wind farm controller then evaluates the total available power from the wind farm by adding all the available powers and finds individual power commands to wind turbines to maximize the wind farm power as shown in Equation (6).

It is a function minimization problem to find power commands to wind turbines to maximize the total power output, and the wind farm model is used for the function minimization process. In Equation (6), J is the objective function to be used for the function minimization process.

$$J = \left|\mathrm{TSO}_{\mathrm{CMD}} - \sum \mathrm{WFC}_{\mathrm{gen},i}\right| \tag{6}$$

The function minimization algorithm is an optimization algorithm that finds optimal variable values that can minimize the objective function consisting of a single or multiple variables. Any function minimization algorithms can be used, but, in this study, the Nelder–Mead simplex algorithm was used for convenience in coding. The algorithm is a multidimensional unconstrained optimization algorithm for nonlinear optimization problems. In addition, it is one of the most widely used function minimization algorithms as a direct search method. The method uses a simplex known as a polytope which has $n + 1$ vertices (or $n + 1$ test points) in n variables of objective function. To find the values that can minimize the objective function value, the method repeats reflection, contraction and expansion of the variables [30,31] by comparing function values at $n + 1$ test points and by avoiding the test point that gives the worst function value. More explanation to understand the algorithm is available in [32].

In this study, the $\mathrm{TSO}_{\mathrm{CMD}}$ in Equation (6) was chosen to be the rated power of the wind turbine multiplied by the number of wind turbines because the curtailment of the total power from the wind farm by the $\mathrm{TSO}_{\mathrm{CMD}}$ is not considered. In addition, only one variable in the objective function, the power command to the most upstream wind turbine, was used to avoid the convergence at a local minimum. In this case, therefore, minimizing the objective function in Equation (6) means that the wind farm controller finds the optimal power command to the most upstream wind turbine to maximize the total power output (from three wind turbines) because the $\mathrm{TSO}_{\mathrm{CMD}}$ will be always larger than the available power from the wind farm except the case when the wind speed is high enough to make all three wind turbines generate at their rated powers.

The wind farm model in the wind farm controller was constructed to calculate the total power output from the wind farm for various operating conditions of the most upstream wind turbine and

finally to find the optimal power regulation of the most upstream wind turbine by minimizing the objective function, Equation (6), using a function minimization algorithm. Basically, the wind farm model predicts the wind speeds for all downstream wind turbines using Ainslie's eddy viscosity wake model and estimates the power output and load variation according to the power command from the power command calculator to maximize the power output by minimizing the objective function. Changes based on the TSO_{CMD} are calculated for all wind turbines. The wind farm model in the wind farm controller is a simplified version of the wind farm model for dynamic simulation in Section 2.1.

Figure 3 shows the difference between the wind farm model used for the dynamic farm simulation and the simplified wind farm model applied to the controller. As shown in the figure, the wind farm model applied to the wind farm controller is similar to that used for the dynamic wind farm simulation in a point that the same wake and the wake merge models are applied to predict the wind speed inside the wind farm. However, the wind farm model in the wind farm controller differ from that for the dynamic wind farm simulation because it does not calculate the wind propagation at each time step and only calculates the steady state winds at the rotors of all downstream wind turbines by considering the wake and the wake superposition. Since the time-dependent wind propagation algorithm is not used in the wind farm model of the wind farm controller, a simple look-up table based wind turbine model without any wind turbine dynamics was used.

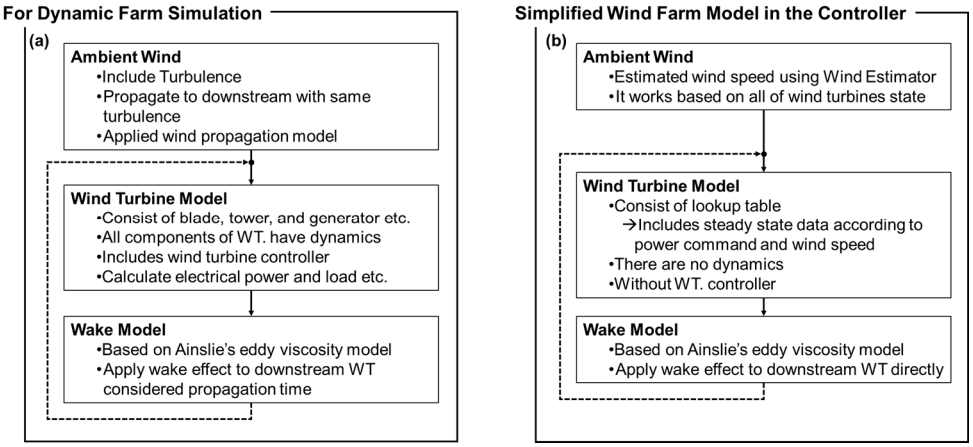

Figure 3. Difference between wind farm simulation tool and wind farm model on wind farm controller: (**a**) structure of dynamic wind farm simulation tool; and (**b**) structure of simplified wind farm model in wind farm controller.

2.3. Wind Turbine Controller

The wind turbine controller in the wind turbine model is based on a comprehensive controller including the MPPT (Maximum Power Point Tracking) torque control for the below rated wind speed region, collective pitch PI control for the above rated wind speed region, and a driver-train damper to reduce the in-plain torsional mode. The MPPT torque control is for power maximization and the collective pitch control is for power regulation to the rated power. For a given generator speed (related to the wind speed), the blade pitch angle and the generator torque must be a constant value to achieve the power maximum or the power regulation. When the wind speed is lower than the rated wind speed, the pitch angle is kept to be the fine pitch known as the pitch angle where the aerodynamic conversion efficiency of the rotor is maximized. At the same time, the generator torque that can achieve the maximum power is commanded from the wind turbine controller to the generator. When the wind speed is higher than the rated wind speed, the generator torque is kept to be the rated torque, and the blade pitch angle is PI controlled to target the rated generator speed [21]. As the result, the rated power is maintained.

For this study, the wind turbine controller was needed to receive a command from a higher level wind farm controller, and a DPPT (demanded power point tracking) control algorithm was constructed and implemented to the basic wind turbine controller. When the power command from the wind farm controller is larger than the available power of the wind turbine, the wind turbine behaves like an ordinary wind turbine with the torque control mode. Thus, if the wind speed is lower than the rated wind speed, the pitch angle is fixed to be the fine pitch and the generator torque command that produces the maximum C_P is sent. If the wind speed is higher than the rated wind speed, the mode switch is turned on to make the wind turbine operate in an ordinary pitch control mode. In this mode, the rated generator toque command and the pitch command to achieve the rated rotational speed are sent from the controller [21].

However, if the power command from the wind farm controller to the wind turbine controller is lower than the available power of the wind turbine, the DPPT control is turned on. The wind turbine controller then sends the generator torque command, which is equivalent to the torque command to achieve the same power output in the ordinary torque control mode. This generator torque is lower than the generator torque needed to achieve the maximum efficiency in the ordinary torque command mode at the same wind speed, and therefore the rotational speed of the generator increases. Now the generator speed, which is equivalent to the generator speed to achieve the same power in the ordinary torque control mode, is targeted in the collective pitch controller. Therefore, in the end, the generator power, which is the generator torque multiplied by the generator speed, is controlled to be the power command from the wind farm controller. The structure of the control algorithm imbedded into the wind turbine controller of the simulation tool without affecting its conventional torque and pitch control logic is shown in Figure 4 [21].

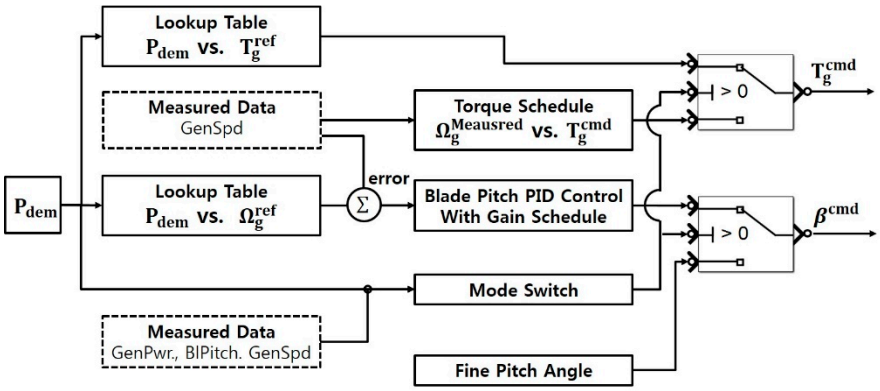

Figure 4. Structure of wind turbine controller [21] Conventional wind turbine controller with torque and pitch control has been modified to have a DPPT control algorithm and to receive power demand from a higher level wind farm controller.

2.4. Simulation

Simulations were performed to see the effect of the wind farm controller. For simulations, three wind turbines in series and aligned to the wind were used. The reason why only three wind turbines were chosen is because, in the previous study, the power regulation of the most upstream wind turbine was found to be mostly effective on the two downstream wind turbines [16].

As a wind turbine, the 5-MW NREL research wind turbine was used. The specification of the wind turbine is shown in Table 1.

The three wind turbines were assumed to be in line with the wind direction and the wind turbine spacing was varied from 4 RD to 10 RD with an interval of 3 RD. In addition, to find the effect of the proposed wind farm control algorithm, only the most upstream wind turbine was used for power regulation to reduce calculation time and avoid convergence in local minimum. The simulation results

were compared with the results with a baseline wind farm controller available in the literature [33,34]. The baseline wind farm control satisfies the command from the transmission system operator when the command is lower than the available power from the wind farm. Each wind turbine receives its share in power generation as a power command, which is proportional to its available power normalized by the total available power in the wind farm. If the command from the TSO is higher than the available power such as the total rated power of the wind farm which is the case considered in this study, the most upstream wind turbine will receive command which is greater than its rated power. As the result, the most upstream wind turbine will extract as much energy from wind as possible, but limited to its rated power by the pitch controller of the wind turbine. The algorithm dispatches power commands to individual wind turbines based on their own available powers, $P_{av,i}$, as shown in Equation (7) [33,34].

$$\mathrm{WFC}_{\mathrm{CMD},i} = \frac{\mathrm{P}_{av,i}}{\sum \mathrm{P}_{av,i}} \times \mathrm{TSO}_{\mathrm{CMD}} \tag{7}$$

Because the wind turbines with more available power (upstream wind turbines) get higher power commands from the wind farm controller, the baseline control is also known as "greedy control". Therefore, it does not consider either the power increase or maximum load reduction in the whole wind farm.

Table 1. Specification of NREL 5-MW wind turbine model [21].

Items	Properties
Rotor, Hub Diameter	126 m, 3 m
Hub Height	90 m
Cut-in, Rated, Cut-out wind speed	3 m/s, 11.4 m/s, 25 m/s
Cut-in, Rated Rotor Speed	6.9 rpm, 12.1 rpm

3. Simulation Result

3.1. Flow Field in Wind Farm

Figure 5 shows snapshots of wind fields obtained from the simulation for two different mean wind speeds with turbulence and with and without the wind farm control. Two different mean wind speeds are 8 m/s and 10.5 m/s. The former is the wind speed lower than the rated wind speed of the wind turbine, and the latter is the wind speed close to the rated wind speed of the wind turbine. The wind is propagating from the left to the right, and therefore the leftmost wind turbine is the most upstream wind turbine. The three short vertical lines represent the turbines. The spacing of wind turbines was 7 RD which is the spacing of the Danish Horns Rev 1 offshore wind farm. The turbulence intensity was 0.075. Because of the turbulence, the wind speed fluctuates and the plots of Figure 5 shows the wind speed distribution at a particular time at which the wind speed at the most upstream wind turbine is 8 m/s (for Figure 5a,c) or 10.5 m/s (for Figure 5e,g).

The two plots in a row such as Figure 5a,b or Figure 5c,d show the wind field in the wind farm, and the steady wind fields normalized by the free stream wind speed, respectively. The latter figure includes numbers above and below the steady wind fields. The former represents the distance in rotor diameter from the most upstream wind turbine and the latter represents the largest wind speed deficit in the wake region. The wind speed deficit increases when the wind speed is further reduced in the wake region. In addition, it reduces as the wind speed in the wake region becomes recovered.

In addition, a set of two rows such as the row with Figure 5a and the row with Figure 5c or the row with Figure 5e and the row with Figure 5g show the results without and with the wind farm control proposed, respectively. In this case, without wind farm control means the greedy control shown in Equation (7), and it is the baseline control used in this study to validate the performance of the proposed wind farm control.

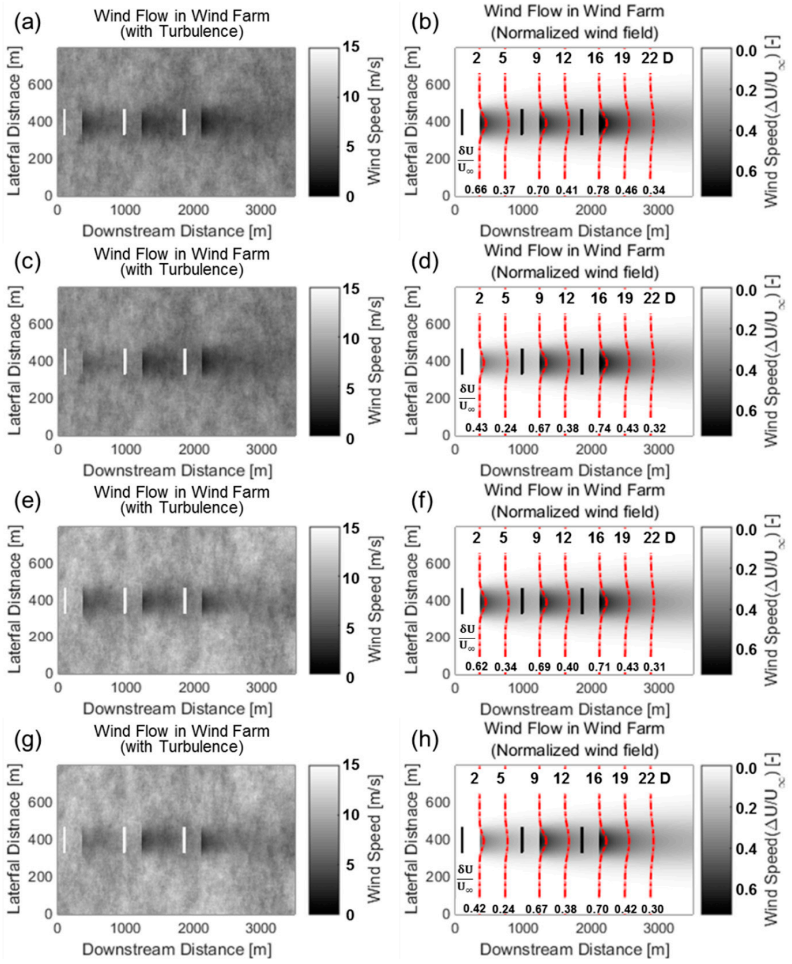

Figure 5. Wind flow variation in wind farm with the baseline and proposed wind farm controllers under ambient turbulence intensity of 0.075: (**a**) turbulent wind field variation with the baseline wind farm control ($\overline{U}$ = 8 m/s); (**b**) steady wind speed deficit of figure (**a**); (**c**) turbulent wind field variation with the proposed wind farm control ($\overline{U}$ = 8 m/s) (**d**) steady wind speed deficit of figure (**c**); (**e**) turbulent wind field variation with the baseline wind farm control ($\overline{U}$ = 10.5 m/s); (**f**) steady wind speed deficit of figure (**e**); (**g**) turbulent wind field variation with the proposed wind farm control ($\overline{U}$ = 10.5 m/s); and (**h**) steady wind speed deficit of figure (**g**). Red dashed line means the wind deficit profile. Deviation from the flat ends represents larger wind speed deficit.

It can be seen in Figure 5a,c that the wake area of the wind turbine is clearly shown in the downstream direction and the influence continues to a relatively long distance. Because the Ainslie's eddy viscosity model neglects the pressure gradient in the near-wake region, the solution is not defined within 2 RD from the upstream wind turbine [25]. Therefore, the wakes begin at 2 RD behind the wind turbine.

In addition, it can be found from the figures that, with the wind farm control (Figure 5c), the wind speed becomes higher in the wake region than the wind speed without the wind farm control. This is because when the wind farm control is turned on, the most upstream wind turbine is forced to generate slightly lower power than the power that it can generate by the wind farm controller. Without the wind farm control (or with the baseline control), the most upstream wind turbine generates electricity with its best. This means that if the farm control is applied to the most upstream wind turbine, the wake impact on the downstream wind turbines is reduced. This is also clearly shown in Figure 5b,d, which shows pure wind speed deficit only in the space excluding the turbulent components of the wind without and with the wind farm control, respectively.

As shown in Figure 5b, where the wind farm control is off, the wake generated between the wind turbines causes significant wind speed reduction, and wake expansion. On the other hand, Figure 5d shows that, if the control is applied to the wind turbine, both effects are much reduced.

With the wind speed of 10.5 m/s, similar effects on the wind flow by the wind farm control can be observed in Figure 5e,g or Figure 5f,h.

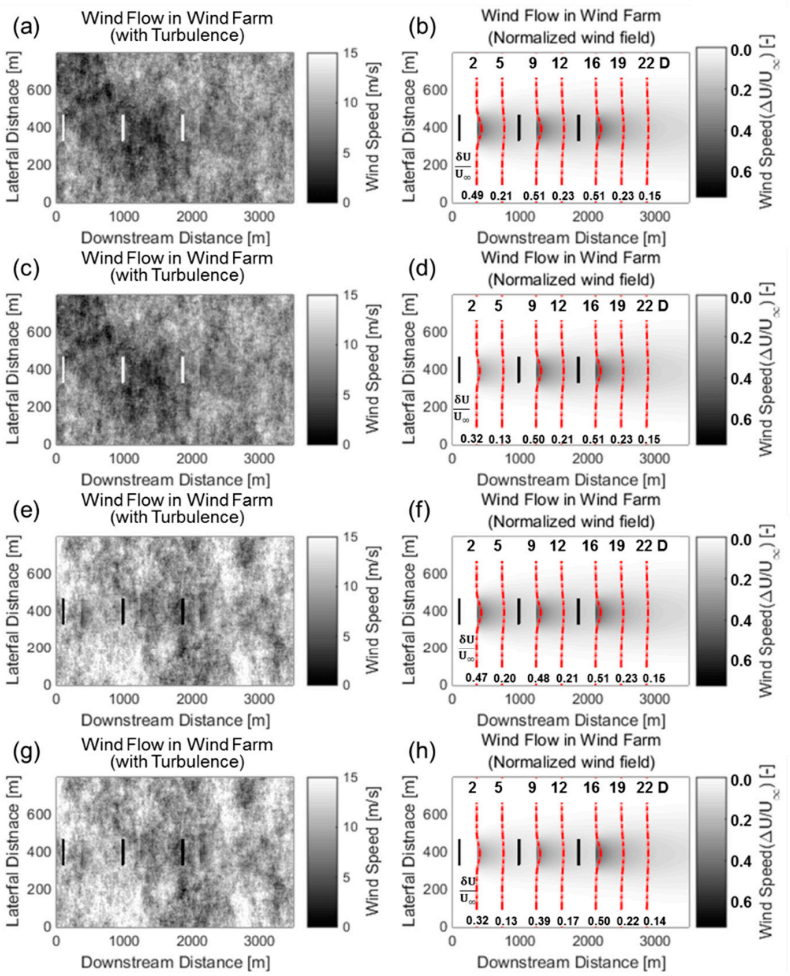

Figure 6. Wind flow variation in wind farm with the baseline and proposed wind farm controllers under ambient turbulence intensity of 0.21: (**a**) turbulent wind field variation with the baseline wind farm control ($\overline{U}$ = 8 m/s); (**b**) steady wind speed deficit of figure (**a**); (**c**) turbulent wind field variation with the proposed wind farm control ($\overline{U}$ = 8 m/s) (**d**) steady wind speed deficit of figure (**c**); (**e**) turbulent wind field variation with the baseline wind farm control ($\overline{U}$ = 10.5 m/s); (**f**) steady wind speed deficit of figure (**e**); (**g**) turbulent wind field variation with the proposed wind farm control ($\overline{U}$ = 10.5 m/s); and (**h**) steady wind speed deficit of figure (**g**). Red dashed line means the wind deficit profile. Deviation from the flat ends represents larger wind speed deficit.

Figure 6 shows exactly the same plots as Figure 5 but with the higher ambient turbulence intensity of 0.21. The higher ambient turbulence intensity can be noticed by severe changes of black and white colors in the figure compared with those in Figure 5. As shown in Figure 6a,c or Figure 6b,d for the mean wind speed of 8 m/s, the wind speed deficit was reduced when the proposed wind farm controller was used. This result is the same as the result of Figure 5. The similar results were obtained for Figure 6e,g or Figure 6f,h that are the cases when the mean wind speed was 10.5 m/s. However, because of the mean wind speed, again, the pitch control was turned on for power regulation, and as the result, the wind speed deficits with the baseline and the proposed controllers were reduced

compared with those at 8 m/s. It is known that the mixing process of the wind becomes more active with the ambient turbulence intensity, and therefore the wake effect is eliminated more quickly compared with Figure 5. As the result, the difference in wind speed deficit with the baseline controller and the proposed controller in Figure 6 was reduced compared with Figure 5.

Figure 7a,b shows the wind speed gain for turbines when the mean wind speed is 8 m/s and the turbulence intensities are 0.075 and 0.21, respectively. As shown in the figure, the input wind speed of all wind turbines located downstream is increased by adjusting the power output of the most upstream wind turbine in both cases. However, as the turbulence intensity increases, the wind speed increase percentage decreases by nearly two times. This phenomenon is related to the wind speed recovery due to the mixing process in the wake region, which is known to be in proportion to the ambient turbulence intensity [25,35]. Since the wind speed in the wake region is rapidly recovered for higher ambient turbulence intensity, the wind speed reduction in the wake region with the baseline controller decreases and finally the wind speed gain with the proposed controller decreases. Figure 7c,d shows the wind speed gain for turbines when the mean wind speed is 10.5 m/s and the turbulence intensities are 0.075 and 0.21, respectively. Because the mean wind speed is close to the rated wind speed of the wind turbine, which is 10.5 m/s, the pitch controller is turned on whenever the wind speed exceeds the rated wind speed. Therefore, the aerodynamic performance of the most upstream wind turbine is reduced to some extent and as the result the power output adjustment of the most upstream wind turbine with the baseline controller becomes less effective on increasing the wind speeds of downstream wind turbines [16].

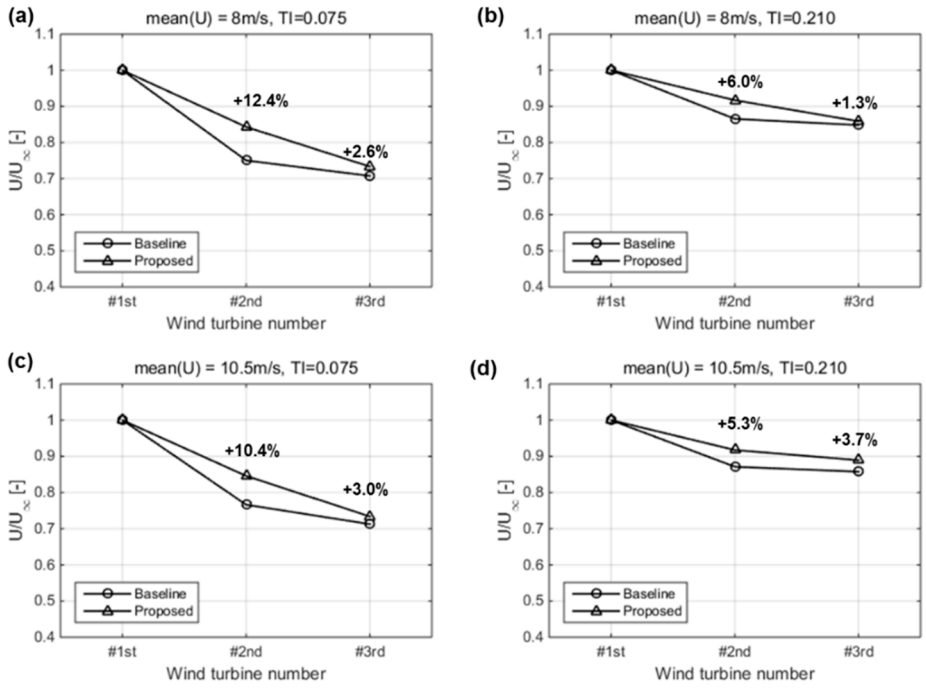

Figure 7. Wind speed variation for downstream wind turbines with the baseline and the proposed wind farm controllers: (**a**) ambient wind speed conditions: $\overline{U}$ = 8 m/s, TI = 0.075; (**b**) ambient wind speed conditions: $\overline{U}$ = 8 m/s, TI = 0.21; (**c**) ambient wind speed conditions: $\overline{U}$ = 10.5 m/s, TI = 0.075; and (**d**) ambient wind speed conditions: $\overline{U}$ = 10.5 m/s, TI = 0.21.

3.2. Total Power

Figure 8 shows the dynamic simulation results with both the baseline controller and the proposed controller. The turbulence intensity was fixed to be 0.075 and the control frequency was 0.1 Hz. The spacing of the wind turbines was 7 RD, which is the turbine spacing of the well-known Danish

Horns Rev offshore wind farm. The mean wind speed to the most upstream wind turbine was fixed to be 8 m/s. Power commands from the wind farm controller to individual wind turbines with both the proposed and the baseline control were calculated from Equations (4) and (5), respectively.

Figure 8a,f shows the turbulent winds to three wind turbines in series. For two different wind farm controllers, the winds to the most upstream wind turbines are the same, but those to the subsequent wind turbines are slightly different. This is because the most upstream wind turbine is operated differently with different wind farm controllers and therefore the winds passing through the turbine are affected differently. Figure 8b,g shows the power commands to individual wind turbines by the wind farm controllers. For the baseline controller, the power command to the most upstream wind turbine is the rated power, 5 MW, and, therefore, the turbine will extract power from the wind as much as possible. The power commands to the downstream two turbines are much lower and dependent on their available powers. For the proposed controller, the power command to the most upstream wind turbine is less than 5 MW to pass slightly more wind to downstream wind turbines. In addition, the power commands to downstream wind turbines are both 5 MW, and therefore the downstream wind turbines will extract power from wind as much as possible.

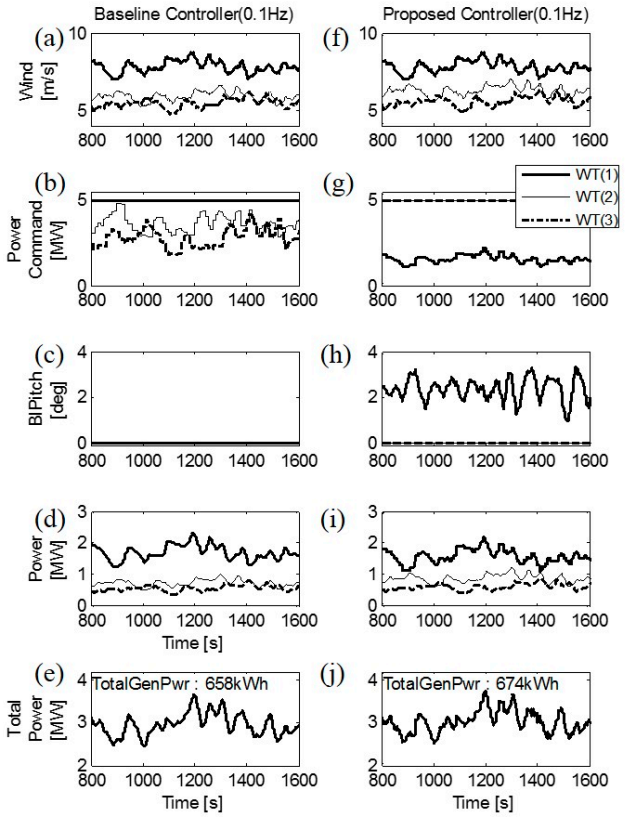

Figure 8. Dynamic simulation results in time domain with baseline and proposed wind farm controllers: (**a**,**f**) wind speed used in comparison of baseline controller and proposed controller for three wind turbines; (**b**,**g**) power command according to use of baseline controller and proposed controller to each wind turbine (**c**,**h**) blade pitch angle change of each wind turbine according to use of baseline controller and proposed controller; (**d**,**i**) generated power variation of wind turbines according to use of baseline controller and proposed controller ; and (**e**,**j**) total power variation of wind farm according to use of baseline controller and proposed controller.

The blade pitch angles are presented in Figure 8c,h. For the baseline controller, the blade pitch angles are zero (fine pitch angle), and no blade pitch control is used. This is because the turbulent wind does not reach the rated wind speed of the wind turbine. All three wind turbines extract as much

power from wind as possible. For the proposed controller, the pitch angles of the two downstream wind turbines are zero, but the pitch angle of the most upstream wind turbine varies within 0° and 4°. This is because the most upstream wind turbine is slightly pitched to pass more wind to downstream wind turbines and the downstream wind turbines do their best to extract power from wind. This result is similar to the result obtained from a wind tunnel with miniature wind turbines with fixed blade pitching by other researchers that the pitch angle of 2° was the best to maximize the wind farm power [4,7]. However, the optimum pitch angle found in this study was not fixed to be 2° but varied with wind speeds or available power.

In the frequency domain analysis, it is known that most energy components in turbulent winds are included within 1 rad/s, and therefore the bandwidth of the pitch controller is commonly chosen to be around or higher than 1 rad/s to cover the wind speed variations [36]. In addition, the bandwidth of the pitch actuators is commonly higher than 100 rad/s, and therefore, as shown in Figure 8b,h, the pitch actuator responds rapidly according to the wind speed variations [21].

Figure 8d,i shows the electrical power generated from the wind turbines for both baseline and proposed wind farm controllers. For the most upstream wind turbines, one with the proposed control generates slightly less power than the other with the baseline control. However, for the two downstream wind turbines, those with the proposed controller generate more than those with the baseline controller. In the end, for the total power, the proposed wind farm controller yields more power than the baseline controller, as shown in Figure 8e,j.

3.3. Tower Load

Figure 9 shows the simulation results for the tower load. More specifically, the load is the fore–aft bending moment at the tower bottom. The mean wind speed, turbulent intensity, control frequency, and the turbine spacing were 8 m/s, 0.075, 0.1 Hz, and 7 RD, respectively. Figure 9a,c shows the dynamic tower loads in the time domain for three wind turbines with the baseline controller and the proposed controller, respectively. As can be seen from the figures, the most upstream wind turbine, regardless of wind farm controllers, experiences the most tower load. In addition, it is shown that with the proposed wind farm controller, the dynamic tower load of the most upstream wind turbine has been substantially reduced. Figure 9b,d shows the loads expressed in DEL (damage equivalent load) to express the fatigue load by periodic loads in a constant value for comparison. The DEL is mathematically defined as

$$\mathrm{D_{eq}} = \left(\frac{\sum_k n_k S_k^m}{\mathrm{N_{eq}}} \right)^{\frac{1}{m}} \tag{8}$$

In Equation (8), S_k is the stress of the tower load having the kth magnitude out of the total tower load during a specified evaluation (simulation) time (commonly 600 s), n_k is the number of cycle of S_k and $\mathrm{N_{eq}}$ is the equivalent number of cycle of $\mathrm{D_{eq}}$ which is commonly calculated from the evaluation (simulation) time multiplied by a frequency of 1 Hz. In addition, in Equation (8), m is a constant related to the slope of the SN (stress to cycles to failure) curve of a material. For a steel tower, the value of 3.5 is used as m [36].

With the baseline wind farm controller, the most upstream wind turbine has the highest load, and it is about 417 kN m. However, with the proposed wind farm controller, the most upstream wind turbine is commanded to generate power slightly less than that the wind turbine can actually generate. Therefore, the most upstream wind turbine passes more wind to downstream wind turbines. As the result, the load of the most upstream wind turbine decreased to 347 kN m.

However, the loads of two downstream wind turbines with the baseline controller, which were 260 kN m and 226 kN m, increased to 285 kN m and 236 kN m with the proposed controller. Although the loads of the two downstream wind turbines increase, they are small compared to the load of the most upstream wind turbine. Therefore, the largest load with the proposed controller becomes lower than the largest load with the baseline controller. The load reduction with the proposed

controller was not targeted in the proposed wind farm control but it can be automatically achieved by reducing the power generation of the most upstream wind turbine. As the result, the proposed wind farm controller is found to levelize the load distribution of wind turbines to some extent in the wind farm.

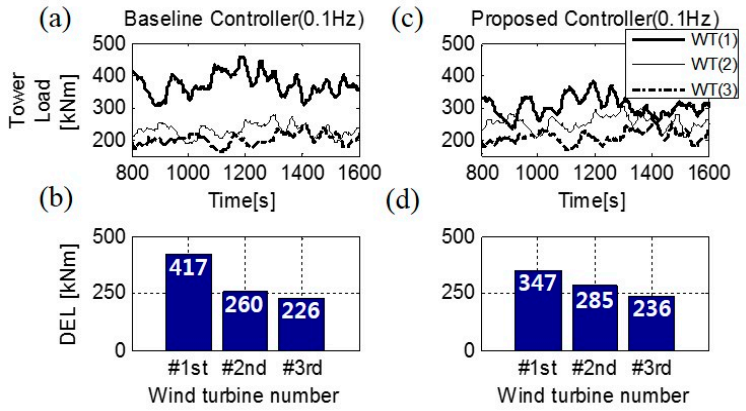

Figure 9. Simulation Result for Load (**a**,**c**) wind turbine tower load variation in time domain when applying baseline controller and proposed controller; (**b**,**d**) wind turbine tower DEL variation when applying baseline controller and proposed controller.

4. Discussion

To fully understand the proposed wind farm control, parametric studies for turbine spacing, turbulent intensity and control frequency were made.

4.1. Total Power

Figures 10 and 11 show the power increase of the proposed wind farm control in percentage relative to the power of the baseline control for two different mean wind speeds, 8 m/s, and 10.5 m/s. Figure 10a,b presents 8 m/s, and Figure 11a,b presents 10.5 m/s. Two wind speeds were chosen for simulation because they correspond to two different wind turbine control regions. The former is the control region for maximum power coefficient and the latter is the control region for smooth transition from the maximum power coefficient control and the rated power control. Based on the figure, it can be found that the power increase of the proposed controller with respect to the power with the baseline controller decreases with increasing wind turbine spacing and increases with increasing control frequency. In addition, the power increase decreased when the ambient turbulent intensity increased. This is partly because more fluctuations in wind speed make the power commands to the wind turbines deviate more from the optimal values. In addition, this is because, with the higher turbulence intensity, the wake recovers more rapidly, and, therefore, the wake loss with the baseline controller is reduced and finally the effect of active induction control is reduced. The power increase was reduced when the wind speed is in the transition control region. When the turbine spacing reached 10 RD, no power increase was observed. It is because when the turbine spacing is 10 RD, the wake loss due to the upstream wind turbine is small. In addition, when the turbulence intensity was large such as 0.21, the power with the proposed control became even lower than the power with the baseline controller when the control frequency was 0.01 or 0.05. This is because the wind farm controller runs too slow to effectively track the high wind speed variation.

However, when the control frequency was 0.1 Hz, although the ambient turbulence intensity was 0.21, the power with the proposed control became higher again than the power with the baseline control. When the turbine spacing was 7 RD the increase was 2.29%. In the previous study with an extremum seeking control [15], a similar decreasing trend in the power gain relative to the baseline control was observed with increasing ambient turbulent intensity, but, with the ambient turbulence

intensity of 0.21, the controller failed to distinguish the change in power by control from the change in power by turbulence, and the power gain became negative.

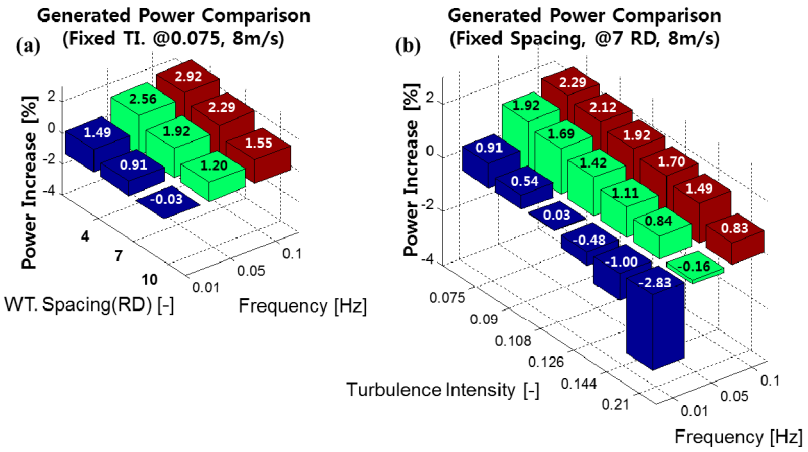

Figure 10. Simulation Results for Power at 8 m/s: (**a**) power increase with wind farm control frequency and wind turbine spacing (fixed condition: TI = 0.075, U = 8 m/s), (**b**) power increase change with wind farm control frequency and ambient turbulence intensity (fixed condition: spacing = 7 RD, U = 8 m/s).

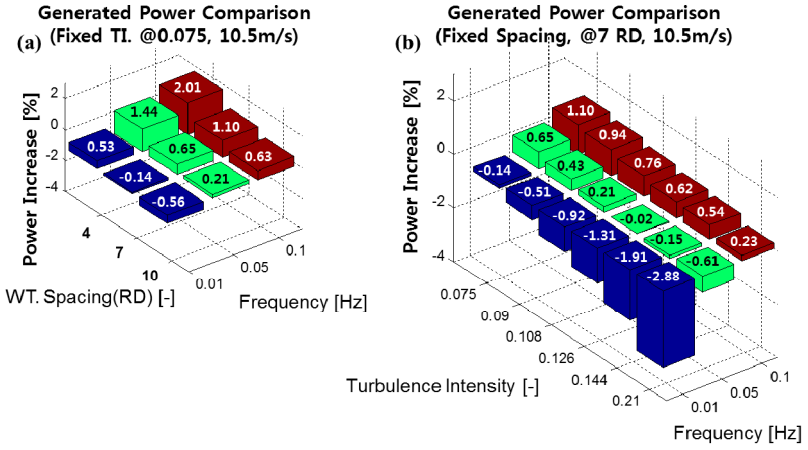

Figure 11. Simulation Results for Power at 10.5 m/s: (**a**) power increase with wind farm control frequency and wind turbine spacing (TI = 0.075, U = 10.5 m/s), (**b**) power increase with wind farm control frequency and ambient turbulence intensity (spacing = 7 RD, U = 10.5 m/s).

4.2. Tower Load

Figure 12 shows the variation of tower load with respect to the turbulence intensity and the control frequency. It is the result when the turbine spacing is 7 RD. As shown in the figure, for all the cases, the tower load of the most upstream wind turbine decreased dramatically.

Although the loads of the downstream wind turbines increased, they were kept lower than the load of the most upstream wind turbine. However, as the control frequency increased from 0.01 Hz to 0.1 Hz, the tower load increased. This is because the wind turbine uses more pitch action with higher control frequency. In addition, it can be found from the figure that the decrease in tower load of the most upstream wind turbine decreases with increasing ambient turbulent intensity. When the ambient turbulence intensity was 0.21, the decrease from the value of the baseline controller was 9.2%. The reason why the tower load increases with the ambient turbulent intensity is because more pitching action occurs in the blade of the wind turbine.

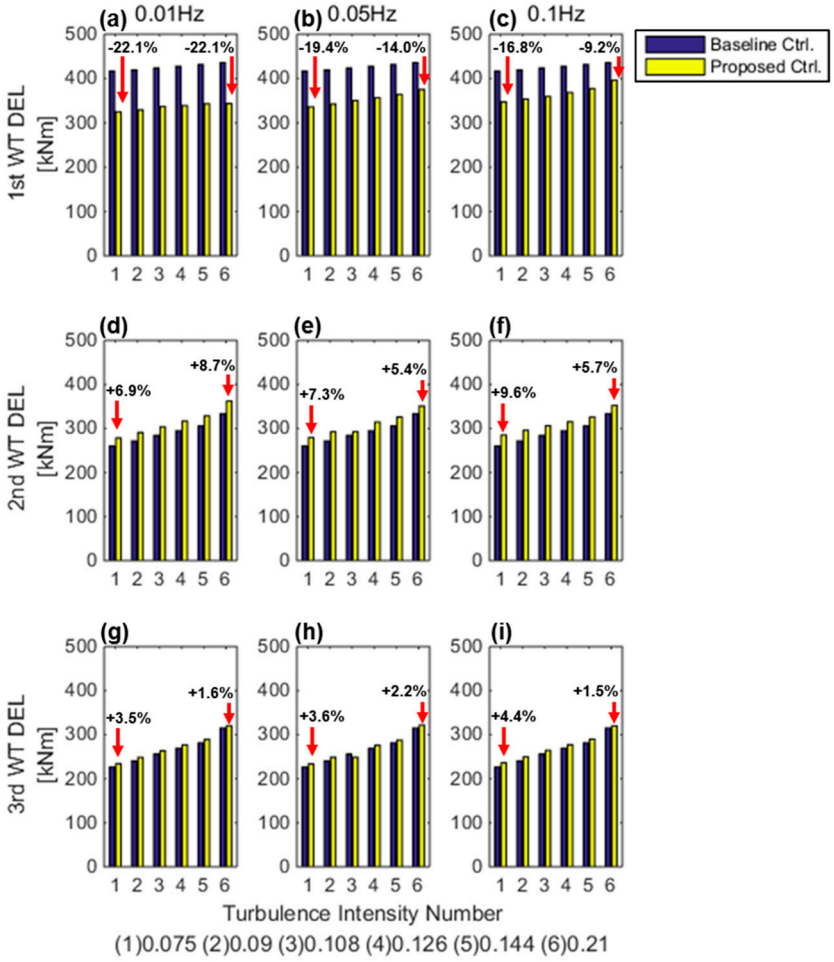

Figure 12. Simulation Results for Tower Load Variation: (**a**–**c**) DEL variation of the first wind turbine according to turbulence intensity and control type(@wind farm control frequency: 0.01, 0.05, 0.1 Hz); (**d**–**f**) DEL variation of the second wind turbine according to turbulence intensity and control type(@wind farm control frequency: 0.01, 0.05, 0.1 Hz) (**g**–**i**) DEL variation of the third wind turbine according to turbulence intensity and control type(@wind farm control frequency: 0.01, 0.05, 0.1 Hz).

4.3. Comparison of Other Models

Table 2 shows the experimental and simulation results of wind farm control available in the literature for comparison. A few experimental results are available in the literature. Based on the table, the results from the experiment showed 4.5–5% increase in power with the manual blade pitching of 2°. However, more experimental validation seems necessary for a concrete conclusion. The simulation results using the Jensen linear wake model showed relatively high power increase. They were 10.57% increase with an optimal control and 6.24% increase with a manual adjustment of the tip speed ratio (TSR). The simulation results with more advanced wake models based on Parabolic Reynolds averaged Navier–Stokes equation (RANS) such as Ainslie's eddy viscosity model or UPMWAKE showed the power increase from 2.85% to 4.5% depending on the turbine spacing and the control type. The power increases were slightly lower than those from the Jensen wake model because the Jensen model with the wake decay constant of 0.04 (recommend for offshore application) is known to be equivalent to the ambient turbulence intensity of approximately 8–10%. Therefore, the wake recovery with the Jensen model is expected to be faster than the wake recovery in the location where the turbulence intensity is lower than. The results from the LES simulation with an actuator disk or an actuator line method showed some discrepancy. The manual blade pitching with the LES simulation showed the power decreases of −2.2% and −8.9% with the blade pitching angle of 2°. The largest decrease in the power

was obtained with five wind turbines in series and, with the blade pitching of the most upstream wind turbine, the power outputs from the four upstream wind turbine were all decreased and the power of the fifth wind turbine was slightly increased compared with the reference baseline control. The reason for this unusual result is explained to be due to the wake meandering effect by the authors of the literature. Unlike the two results with the LES simulation, the optimal control algorithm applied to the LES simulation with an actuator disk model showed the power increase of 16%. However, the wind turbine control algorithms and wind turbine dynamics were not used in the study and this might reduce the power increase. Although the results in Table 2 were obtained with different conditions and cannot be compared directly, the results in this study with the proposed model predictive open loop wind farm control are within the range of the results obtained from other studies, and the power gains are relatively low. The reason for this is considered to be that more realistic conditions including wind turbine dynamics, wind turbine control, and wind farm control frequency have been added in the simulation of this study. However, experimental study must be done as a future work to fully validate the result.

4.4. Strengths and Weaknesses of the Current Study

The strengths of the current study can be summarized as the following two points. First, the current study considered the actual application of the wind farm control algorithm to the real wind farm, and proposed a simple but effective open loop wind farm control which can be fully applied to a wind farm controller (hardware) and used without affecting the current wind turbine control algorithms. The wind farm controller receives the measured generator speed, blade pitch angle, and the power output from the wind turbine controller and sends the optimal power command to the wind turbine controller.

In addition, the proposed wind farm control algorithm is validated in a relatively high-fidelity wind farm simulation tool [20], which has wind turbine dynamics and control including the basic torque and pitch controller slightly modified to include the demanded power point tracking (DPPT) control [37]. Therefore, the current wind farm simulation is almost the same as the real wind farm in terms of control. In addition, the wind farm control frequency applied was at least 10 times slower than the wind variation in the simulation to get more realistic simulation results. Parametric studies including turbulence intensities, turbine spacing and wind farm control frequencies were made to see the effects of active induction control on the total power increase in some more detail.

This study also has some weaknesses and they are as follows. The wake model used in this study is Ainslie's eddy viscosity model which uses the thin boundary layer approximation on the RANS (Reynolds Averaged Navier–Stokes) equation with the empirical boundary condition obtained from the wind tunnel test. Although the model or its modified version is commonly used in commercial software for calculating the power outputs of a single or multiple wind turbines including the wake effect, the accuracy of the model needs to be experimentally validated with various wind turbine operating conditions.

In addition, in this study, the wake meandering is not considered. If the meandering is considered, the power decrease in the wake region might be changed and, therefore, the performance of the proposed wind farm control algorithm will be affected. Therefore, in the future, experimental validation of the simulation results needs to be performed.

Table 2. The Trend of Active Wake Control Validation (RD: rotor diameter, TSR: tip speed ratio, Pav: available power, WT: wind turbine, DPPT: demanded power point tracking).

Researcher	Wind Farm Model	Wind	Spacing	Induction Control Type	Power Increase
Boorsma K. [7]	- Real wind farm - WT. model: Full size (2.5 MW)	Turbulent	3.5 RD	- Manual Pitch	+5.00% @2°
Corten G.P. [5]	- Wind Tunnel - WT model: Scaled model	Turbulent	4.5 RD	- Manual Pitch	+4.50% @2°
De-Prada-Gil M. [8]	- Jensen wake model - WT. model: BEM (no WT. dynamics)	Constant	7.0 RD	- Manual TSR	+6.24%
Behnood A. [9]	- Jensen wake model - WT. model: BEM (no WT. dynamics)	Turbulent	3.3 RD	- Optimal algorithm	+10.57%
Lee J. [10]	- Ainslie wake model - WT. model: BEM (no WT. dynamics)	Constant	7.0 RD	- Optimal Algorithm	+4.50%
Kim H. [16]	- Ainslie wake model - WT. model: BEM (include WT. dynamics &control)	Constant	4.0 RD	- Manual Power Command	+4.10% @0.825 × P_{av}
Horvat T. [11]	- UPMWAKE - WT. model: BEM (no WT. dynamics)	Constant	3.2 RD	- Optimal Algorithm	+2.85%
Clevenhult T.A. [12]	- Madjidian and Rantzer - WT. model: BEM (with WT. dynamics & control)	Turbulent	5.0 RD	- Optimal Algorithm	+3.26%
Nilsson K. [17]	- Large Eddy Simulation - WT. model: Actuator disk	Turbulent	3.3 RD4.3 RD	- Manual Pitch	−2.20% @2°
Annoni J. [18]	- Large Eddy Simulation - WT. model: Actuator Line coupled with FAST	Turbulent	5.0 RD	- Manual Pitch	Approx. −8.90% @2°
Goit J.P. [19]	- Large Eddy Simulation - WT. model: Actuator disk	Turbulent	4.0 RD	- Optimal Algorithm	+16.00%
Current Study	- Ainslie wake model - WT. model: BEM (with WT. dynamics & control including DPPT)	Turbulent	4.0 RD~10.0 RD	- Optimal Algorithm	+2.92% @4 RD +2.29% @7 RD +1.55% @10 RD

5. Conclusions

A simple but effective model based open-loop wind farm control algorithm was proposed and validated with a relatively high-fidelity simulation tool in this study. The wind farm model for control was a simplified version of the wind farm model for dynamic simulation, and consisted of a wind turbine model, wake model, wind propagation and superposition model, and a wind farm control model. Unlike the wind farm model for simulation, it had a look-up table based wind turbine model that does not have wind turbine dynamics. The wind farm model was used in the wind farm controller to find optimal power commands to individual wind turbines. With a function minimization algorithm, the wind farm control algorithm was validated with dynamic simulations with turbulent winds. For a virtual wind farm with three wind turbines in series, simulations were performed for both the baseline and the proposed wind farm controllers at the mean wind speed of 8 m/s. As the result, the proposed wind farm controller was found to increase the total power output by about 2.4% and to decrease the load of the most upstream wind turbine in DEL by about 16.7% when the turbulence intensity was 0.075 and the control frequency was 0.1 Hz.

In addition, parametric studies were performed to understand the power increase of the proposed wind farm controller compared with the baseline controller for different turbulent wind speeds different turbulence intensities and different control frequencies. The power increase was found to decrease as the turbine spacing increases and it decreased to about 1.5% when the turbine spacing was 10 RD at the mean wind speed of 8 m/s. In addition, the power increase was found to decrease as the turbulence intensity increases and it decreased to about 0.83% when the turbulence intensity was increased to 0.21. When the mean wind speed was close to the rated wind speed, the power increase was also found to decrease.

Although no wind direction change was considered in the current study, the effect of the model based wind farm control algorithm was found to be effective to increase power and reduce load in a wind farm. However, in the current study, the Ainslie's eddy viscosity wake model was used to calculate the wind speed in the wake region, and Taylor's frozen turbulence assumption was used for wind speed propagation. Therefore, the results need to be experimentally validated in a wind tunnel or in the field for better understanding.

Acknowledgments: This work was supported by the Human Resources Program in Energy Technology and New & Renewable Energy Core Technology program of the Korea Institute of Energy Technology Evaluation and Planning (KETEP) granted financial resource form the Ministry of Trade, Industry & Energy, Korea (Nos. 20154030200950 and 20153030023610).

Author Contributions: H.K. developed wind farm simulation tool and farm controller; K.K. constructed wind turbine model and developed wind turbine controller; and I.P. and H.K. analyzed simulation results and wrote the paper.

Conflicts of Interest: The authors declare no conflict of interest.

References

1. Rodrigues, S.; Restrepo, C.; Kontos, E.; Pinto, R.T.; Bauer, P. Trends of offshore wind projects. *Renew. Sustain. Energy Rev.* **2015**, *49*, 1114–1135. [CrossRef]
2. 4C Offshore. Offshore Wind Farms. Available online: www.4coffshore.com/windfarms (accessed on 1 June 2017).
3. Barthelmie, R.J.; Pryor, S.; Frandsen, S.T.; Hansen, K.S.; Schepers, J.; Rados, K.; Schelez, W.; Neubert, A.; Jensen, L.E.; Neckelmann, S. Quantifying the impact of wind turbine wakes on power output at offshore wind farms. *J. Atmos. Ocean. Technol.* **2010**, *27*, 1302–1317. [CrossRef]
4. Gustave, P.C.; Pieter, S. Heat and flux: Increase of wind farm production by reduction of the axial induction. In Proceedings of the European Wind Energy Conference, Madrid, Spain, 16–19 June 2003.
5. Corten, G.P.; Schaak, P. More power and less loads in wind farms. In Proceedings of the European Wind Energy Conference, London, UK, 22–25 November 2004.

6. Machielse, L.A.H.; Barth, S.; Bot, E.T.G.; Hendriks, H.B.; Schepers, G.J. *Evaluation of 'Heat and Flux' Farm Control*; Technical Report ECN-E-07-105; Energy Research Centre of the Netherlands: Petten, The Netherlands, 2007.
7. Boorsma, K. *Heat and Flux—Analysis of Field Measurements*; ECN Report, ECN-E-12-048; Energy Research Centre of the Netherlands: Petten, The Netherlands, 2012.
8. De-Prada-Gil, M.; Alias, C.G.; Gomils-Bellmunt, O.; Sumper, A. Maximum wind power plant generation by reducing the wake effect. *Energy Convers. Manag.* **2015**, *101*, 73–84. [CrossRef]
9. Behnood, A.; Gharavi, H.; Vahidi, B.; Riahy, G.H. Optimal output power of not properly designed wind farms, considering wake effects. *Electr. Power Energy Syst.* **2014**, *63*, 44–50. [CrossRef]
10. Lee, J.; Son, E.; Hwang, B.; Lee, S. Blade pitch angle control for aerodynamic performance optimization of a wind farm. *Renew. Energy* **2012**, *54*, 124–130. [CrossRef]
11. Horvat, T.; Spudić, V.; Baotić, M. Quasi-stationary optimal control for wind farm with closely spaced turbines. In Proceedings of the MIPRO 2012, Opatija, Croatia, 21–25 May 2012; pp. 829–834.
12. Thomas, A.C.; Fredirik, H. Added Turbulence and Optimal Power Distribution in Large Off-Shore Wind Farms. Master's Thesis, Lund University, Lund, Sweden, 2010.
13. Jason, R.M.; Shalom, D.R.; Lucy, Y.P. A model-free approach to wind farm control using game theoretic methods. *IEEE Trans. Control Syst. Technol.* **2013**, *21*, 1207–1214. [CrossRef]
14. Gebraad, P.M.O.; van Dam, F.C.; van Wingerden, J.-W. A model-free distributed approach for wind plant control. In Proceedings of the 2013 American Control Conference (ACC), Washington, DC, USA, 17–19 June 2013; pp. 628–633.
15. Johnson, K.E.; Fritsch, G. Assessment of extremum seeking control for wind farm energy production. *Wind Eng.* **2012**, *36*, 701–716. [CrossRef]
16. Kim, H.; Kim, K.; Paek, I. Power regulation of upstream wind turbines for power increase in a wind farm. *Int. J. Precis. Eng. Manuf.* **2016**, *17*, 665–670. [CrossRef]
17. Nilsson, K.; Ivanell, S.; Hansen, K.S.; Mikkelsen, R.; Sørensen, J.N.; Breton, S.; Henningson, D. Large-eddy simulations of the Lillgrund wind farm. *Wind Energy* **2013**, *18*, 449–467. [CrossRef]
18. Annoni, J.; Gebraad, P.M.O.; Scholbrock, A.K.; Fleming, P.A.; Wingerden, J. Analysis of axial-induction-based wind plant control using an engineering and a high-order wind plant model. *Wind Energy* **2016**, *19*, 1135–1150. [CrossRef]
19. Goit, J.P.; Meyers, J. Optimal control of energy extraction in wind-farm boundary layers. *J. Fluid Mech.* **2015**, *768*, 5–50. [CrossRef]
20. Kim, H.; Kim, K.; Paek, I.; Yoo, N. Development of a time-domain simulation tool for offshore wind farms. *J. Power Electron.* **2015**, *15*, 1047–1053. [CrossRef]
21. Jonkman, J.; Butterfield, S.; Musial, W.; Scott, G. *Definition of a 5-MW Reference Wind Turbine for Offshore System Development*; Technical Report NREL/TP-500-38060; National Renewable Energy Laboratory: Golden, CO, USA, 2009.
22. Cheng, M.; Shu, Y. The state of the art of wind energy conversion systems and technologies: A review. *Energy Convers. Manag.* **2014**, *88*, 332–347. [CrossRef]
23. Zhu, Y.; Cheng, M.; Hua, W.; Wang, W. A novel maximum power point tracking control for permanent magnet direct drive wind energy conversion systems. *Energies* **2012**, *5*, 1398–1412. [CrossRef]
24. Jacob, D.G.; Soltani, M.N.; Torben, K.; Martin, N.K.; Thomas, B. Aeolus toolbox for dynamics wind farm model, simulation and control. In Proceedings of the European Wind Energy Conference and Exhibition (EWEC), Warsaw, Poland, 20–23 April 2010.
25. Ainslie, J.F. Calculating the flowfield in the wake of wind turbines. *J. Wind Eng. Ind. Aerodyn.* **1988**, *27*, 213–224. [CrossRef]
26. Nielsen, P.; EMD International A/S. *WindPRO User Guide*; EMD International A/S: Aalborg, Denmark, 2012.
27. Göçmen, T.; Laan, P.; Réthoré, P.E.; Diaz, A.P.; Larsen, G.C.; Ott, S. Wind turbine wake models developed at the technical university of Denmark: A review. *Renew. Sustain. Energy Rev.* **2016**, *60*, 752–769. [CrossRef]
28. Kim, K.; Lim, C.; Oh, Y.; Kwon, I.; Yoo, N.; Paek, I. Time-domain dynamic simulation of a wind turbine including yaw motion for power prediction. *Int. J. Precis. Eng. Manuf.* **2015**, *15*, 2199–2203. [CrossRef]
29. Singh, M.; Santoso, S. *Dynamic Models for Wind Turbines and Wind Power Plants*; Subcontract Report NREL/SR-5500-52780; National Renewable Energy Laboratory: Golden, CO, USA, 2011.
30. Nelder, J.A.; Mead, R. A Simplex Method for Function Minimization. *Comput. J.* **1965**, *7*, 308–313. [CrossRef]

31. Rajan, A.; Malakar, T. Optimal reactive power dispatch using hybrid Nelder-Mead simplex based firefly algorithm. *Int. J. Electr. Power Energy Syst.* **2015**, *66*, 9–24. [CrossRef]
32. Nocedal, J.; Wright, S.J. *Numerical Optimization*, 1st ed.; Springer: Berlin, Germany, 2000; pp. 360–391.
33. Kaneko, T.; Yona, A.; Funabashi, T. Output Power Coordination Control for Wind Farm in Small Power System. In Proceedings of the International Conference on Intelligent Systems Applications to Power Systems, Niigata, Japan, 5–8 November 2007; pp. 51–56.
34. Guan, X.; Molen, G.M. *Aeolus Project Deliverable d3.1: Control Strategy Review and Specification (Part 1)*; Technical Report; Industrial Systems and Control: Glasgow, UK, 2009.
35. Jensen, N.O. *A Nnote on Wind Generator Iinteraction*; Risø National Laboratory: Roskilde, Denmark, 1983.
36. Nam, Y. *Wind Turbine System Control*, 1st ed.; GS Intervision: Seoul, Korea, 2013; pp. 400–401.
37. Kim, K.; Kim, H.; Kim, C.; Paek, I.; Bottasso, C.; Campagnolo, F. Design and validation of demanded power point tracking control algorithm of a wind turbine. *Int. J. Precis. Eng. Manuf. Green Technol.* **2017**, in press.